16th Australasian Fluid Mechanics Conference
Crown Plaza, Gold Coast, Australia
2-7 December 2007

# An Enhanced Characteristic Based Method for Artificially Compressible Flows with Heat Transfer

**M. Azhdarzadeh[1], S.E. Razavi [2]**
**Zh. Azhdarzadeh[3]**

[1, 2] Department of Mechanical Engineering
Tabriz University, Iran, Tabriz, m.azhdarzadeh@gmail.com

[3] Tabriz Azad University (Sama), Iran, Tabriz

## Abstract

The purpose of the current work is to develop a solution method for incompressible Navier-Stokes equations both for velocity and temperature fields based on artificial compressibility concept. The equations are discretized in Finite-Volume formulation, convective fluxes are calculated using a high-order characteristic-based Roe-like flux splitting. For time-marching 5th-order Runge-Kuta algorithm, because of its wide range of stability, is used. The formulation can be used both for steady and unsteady flows. The results for three different flux treatments are presented. The method validation is performed by solving velocity and temperature fields over a ribbed surface and comparing them by experimental data, in which a reasonable agreement would exist. The convergence rate of the method shows a sensible reduction in iteration steps. The influence of semi-hexagonal riblet on local Nusselt number is addressed.

**Keywords**: Artificial Compressibility Method**,** Characteristic Based Method**,** Finite-volume

## Introduction

In the past decade, much progress has been made in developing computational techniques for predicting flow and heat transfer fields. The accuracy and efficiency of these methods can be affected by factors such as flux treatment, boundary conditions and the grid type. Many existing methods have been developed to solve the compressible flow equations within transonic Mach numbers. However, a lot of applied problems, such as those in cooling electronic components are inherently incompressible and must be treated appropriately. With the progress in recent years of the compressible flow schemes, these have naturally been considered for use with incompressible flows simply by lowering the Mach number to minimize compressibility effects. Unfortunately, as Mach number is successively decreased toward incompressible limit, the performance of compressible methods in terms of both convergence rate and accuracy suffers greatly. Volpe [15] demonstrated the poor performance of compressible flow solvers under these conditions, particularly for Mach numbers below approximately 0.1.

To overcome the difficulties associated with the use of compressible methods, excellent progress has been made in applying artificial compressibility method (ACM) to incompressible flows. ACM is a way of extending a compressible flow solver to use at zero Mach numbers, which first introduced by Chorin [2]. The method has been successfully used both for steady and unsteady flows.
Tai et al. [14], have developed a Navier-Stokes solver for velocity field which is based on the artificial compressibility method and in finite-volume discretization. Rogers et al. [13] applied the ACM to unsteady problems with an implicit line-relaxation procedure using finite-difference discretization.
Some researchers have applied ACM in conjunction with different upwind differencing schemes and solution techniques to solve steady-state as well as unsteady incompressible problems. The upwind differencing schemes that have been used include the flux-difference splitting [12], MUSCL [1], TVD [4], and WENO [16], schemes. Kao et al. [7] have used a segregated finite-difference scheme based on ACM to solve velocity field of shear-driven cavity.

As Madsen [9] and McClimans [10] have claimed, the time marching approach used in this work can predict both steady and unsteady flows but this work will focus on steady condition.
Riblets with various geometries find the growing application as heat transfer promoters and also vortex generators. Most of the works in treating two-dimensional riblets devote to the square shapes not for semi-hexagonal riblets which has been treated here.

The purpose of the current work is to develop a solution method for incompressible Navier-Stokes equations both for velocity and temperature fields on the basis of ACM concept in Finite-Volume discretization. In this paper a new second-order algorithm is proposed for advective flux calculation of incompressible flow. Convective fluxes are modeled using a high-order characteristic-based Roe-like flux splitting approach. For time-marching a 5th order Runge-Kuta, because of its wide range of stability is used. The method validation is performed by solving velocity and temperature fields over a ribbed surface and comparing them by experimental data. The influence of riblet on local Nusselt number is discussed. To the authors knowledge, there is no work in literature which uses exactly the numerical procedure used in the current geometry, to solve velocity and temperature fields simultaneously. Most of the works performed on the ribbed surfaces were experimental and usually not in semi-hexagonal geometry [8]. The numerical works have used other procedures and usually were limited to only velocity field [5].

## Governing equations

The primitive form of the incompressible Navier-Stokes equations in Finite-volume form with artificial compressibility reads

$$\iint_{\Omega} \frac{\partial U}{\partial t} dA + \oint_{\partial\Omega} \left(Fdy - Gdx\right) = \frac{1}{\mathrm{Re}} \oint_{\partial\Omega} \left(Rdy - Sdx\right) \tag{1}$$

where

$$U=\begin{bmatrix}p\\u\\v\\\theta\end{bmatrix},\ F=\begin{bmatrix}\beta u\\u^2+p\\uv\\u\theta\end{bmatrix},\ G=\begin{bmatrix}\beta v\\uv\\v^2+p\\v\theta\end{bmatrix},$$
$$R=\frac{1}{\mathrm{Re}}\begin{bmatrix}0\\\frac{\partial u}{\partial x}\\\frac{\partial v}{\partial x}\\\frac{1}{\mathrm{Pr}}\frac{\partial\theta}{\partial x}\end{bmatrix},\ S=\frac{1}{\mathrm{Re}}\begin{bmatrix}0\\\frac{\partial u}{\partial y}\\\frac{\partial v}{\partial y}\\\frac{1}{\mathrm{Pr}}\frac{\partial\theta}{\partial y}\end{bmatrix} \tag{2}$$

Equation 1, has been non-dimensionalized by the following reference values,

$$x=\frac{\hat{x}}{h},\ y=\frac{\hat{y}}{h},\ t=\frac{\hat{t}}{h/u_\infty},\ p=\frac{\hat{p}-p_\infty}{\rho u_\infty^2},\ u=\frac{\hat{u}}{u_\infty},\ v=\frac{\hat{v}}{u_\infty}$$
$$\theta=\frac{T-T_\infty}{T_w-T_\infty},\qquad \mathrm{Re}=\frac{u_\infty h}{\nu},\qquad \mathrm{Pr}=\frac{\alpha}{\nu} \tag{3}$$

**Convective Flux Treatment**

At the present time various flux treatments are in use. The averaging method is widely employed in the literature. Here a characteristic-based Roe-like approach is developed to compute convective fluxes at the cell boundaries. By the aid of ACM, the governing equations took a hyperbolic dominated nature, therefore the application of characteristic based wave propagation models would become possible. Roe method has been originally developed to estimate the fluxes of Euler equations [11] but in current work a similar approach is applied to the artificial compressible system of Navier-Stokes equations. In this method fluxes at cell boundary are written as:

$$Flux=\frac{1}{2}\left(NF_R+NF_L\right)-\frac{1}{2}|A|\left(U_R-U_L\right) \tag{4}$$

Where, $NF$ is the flux vector normal to the grid boundaries, $U_R$ and $U_L$ are the values of variables at the right and left side of cell boundaries and

$$|A|=R|\Lambda|L \tag{5}$$

Where $\Lambda$ is a diagonal matrix, whose elements are the eigen-values of flux jacobian matrix A, and are given by

$$\begin{aligned}\lambda_1&=N+c\\\lambda_2&=N-c\\\lambda_3&=N\end{aligned} \tag{6}$$

Where

$$N=n_x u+n_y v \tag{7}$$
$$c=\sqrt{N^2+\beta} \tag{8}$$

$R$ and $L$ are right and left eigenvectors of matrix $A$ respectively. These matrices for the primitive variables, in the presence of artificial compressibility factor has been derived as follows,

$$R=\begin{bmatrix}0 & \frac{\beta c}{N+c} & -\frac{\beta c}{N-c}\\ -\frac{n_y}{n_x} & n_x c-n_y\varphi & -(n_x c+n_y\varphi)\\ 1 & n_x\varphi+n_y c & n_x\varphi-n_y c\end{bmatrix} \tag{9}$$

$$L=\begin{bmatrix}-\frac{\varphi n_x}{c^2} & -\frac{(v\theta+n_y\beta)n_x}{c^2} & \frac{(u\theta+n_x\beta)n_x}{c^2}\\ \frac{1}{2c^2} & \frac{1}{2}\frac{(\theta+c)n_x}{c^2} & \frac{1}{2}\frac{(\theta+c)n_y}{c^2}\\ \frac{1}{2c^2} & -\frac{1}{2}\frac{(-\theta+c)n_x}{c^2} & -\frac{1}{2}\frac{(-\theta+c)n_y}{c^2}\end{bmatrix} \tag{10}$$

Where $\varphi$ is the shear velocity,

$$\varphi=n_x v-n_y u \tag{11}$$

These results lead to the following $|A|$ matrix,

$$|A|=\begin{bmatrix}a_{1,1} & a_{1,2} & a_{1,3}\\a_{2,1} & a_{2,2} & a_{2,3}\\a_{3,1} & a_{3,2} & a_{3,3}\end{bmatrix} \tag{12}$$

where

$$\begin{aligned}
&a_{1,1}=\frac{\beta}{c},\qquad a_{1,2}=\frac{\beta N}{c}n_x,\qquad a_{1,3}=\frac{\beta N}{c}n_y\\
&a_{2,1}=-\frac{n_y\varphi c-n_x N c-n_y\varphi|N|}{c^2}\\
&a_{2,2}=\frac{n_x^2cN^2+n_x^2c^3-2n_xn_y\varphi Nc+n_xn_y\varphi|N|N+n_y^2|N|c^2}{c^2}\\
&a_{2,3}=\frac{n_y(n_xcN^2+n_xc^3-2n_y\varphi Nc+n_y\varphi N|N|-n_x|N|c^2)}{c^2}\\
&a_{3,1}=\frac{n_xc\varphi+n_ycN-n_x|N|\varphi}{c^2}\\
&a_{3,2}=\frac{n_x(n_ycN^2+n_yc^3+2n_xc\varphi N-n_x\varphi N|N|-n_yc^2|N|)}{c^2}\\
&a_{3,3}=\frac{n_y^2N^2c+n_y^2c^3+2n_xn_yc\varphi N-n_xn_y\varphi N|N|+n_x^2c^2|N|}{c^2}
\end{aligned} \tag{13}$$

All the components are calculated using an average of variables in different sides of cell boundary, which reads,

$$U=\frac{U_R+U_L}{2} \tag{14}$$

The order of accuracy of the scheme depends on choosing $U_R$ and $U_L$ values. Assigning cell-center values leads to a first order accuracy, Equation 15, but using a kind of interpolation [3] will result in second order of accuracy, Equation 16,

First-order

$$U_{L,i+1/2}=U_i\ ,\qquad U_{R,i+1/2}=U_{i+1} \tag{15}$$

Second-order

$$U_{L,i+1/2} = \frac{3}{2}U_i - \frac{1}{2}U_{i-1}$$
$$U_{R,i+1/2} = \frac{3}{2}U_{i+1} - \frac{1}{2}U_{i+2} \qquad (16)$$

Since the velocity field is assumed to have constant fluid properties such as viscosity coefficient and density, so velocity field in this case is independent of temperature field. By this assumption, the fluxes related to the velocity field will be treated separately by the use of formulation given in Equation 4. The fluxes of temperature field are computed using an interpolation dependent on the order of accuracy desired. In other words the fluxes related to velocity and temperature fields are treated in two different ways. This kind of treatment has shown better efficiency, at least in current observations.

### Viscous Fluxes

The viscous fluxes discretization is straightforward and uses a kind of 2nd-order averaging. The right hand-side of Equation 1 in discretized form becomes,

$$\text{RHS of Eq. 1} \approx \sum_{i=1}^{m}\left(R_i \Delta y_i - S_i \Delta x_i\right) \qquad (17)$$

In the calculation of $R_i$ and $S_i$, secondary cells are employed.

### Time Discretization Procedure

For marching in time the well known 5th-order Runge-Kuta algorithm of Jameson [6] is utilized. This allows to handle the proposed scheme at higher CFL numbers. The solution is updated at consecutive time steps as shown in Equation 18.

$$\begin{aligned}
&\frac{dU}{dt} + R(U) = 0 \\
&U^{(0)} = U^{(n)} \\
&U^{(1)} = U^{(0)} - \alpha_1 \Delta t R\left(U^{(0)}\right) \\
&U^{(2)} = U^{(0)} - \alpha_2 \Delta t R\left(U^{(1)}\right) \\
&U^{(3)} = U^{(0)} - \alpha_3 \Delta t R\left(U^{(2)}\right) \\
&U^{(4)} = U^{(0)} - \alpha_4 \Delta t R\left(U^{(3)}\right) \\
&U^{(5)} = U^{(0)} - \alpha_5 \Delta t R\left(U^{(4)}\right) \\
&U^{(n+1)} = U^{(5)}
\end{aligned} \qquad (18)$$

Where

$$\alpha_1 = 1/4, \quad \alpha_2 = 1/6, \quad \alpha_3 = 3/8$$
$$\alpha_4 = 1/2, \quad \alpha_5 = 1 \qquad (19)$$

The 5th order Runge-Kuta algorithm has stability margin of CFL= 4 for the linear advective equation. Stability requirement impose a restriction on the time-marching steps [5], to have a stable solution time-marching steps should satisfy the following conditions,

$$\Delta t_{\max} = \frac{CFL \times \Delta L_{\min}}{C_{\max}} \qquad (20)$$

where

$$\begin{aligned}
&C_{i,j} = \sqrt{\beta} + \sqrt{u_{i,j}^2 + v_{i,j}^2} \\
&C_{\max} = Max\left(C_{i,j}\right) \\
&\Delta L_{\min(i,j)} = \sqrt{\left(\Delta x_{i,j}\right)^2 + \left(\Delta y_{i,j}\right)^2} \\
&\Delta L_{\min} = Min(\Delta L_{i,j})
\end{aligned} \qquad (21)$$

### Boundary Conditions

Consistent boundary treatment ensures the disturbance dissipation in discretized domain without reflection. At the solid boundary a condition of zero mass and energy flux through the surface is prescribed by setting the fluxes corresponding to these faces equal to zero. Pressure on the solid surface is found by solving normal momentum equation and temperature on the solid surface is assumed to be constant. This technique only permits a flux of the pressure terms of momentum equation through a solid boundary. At the inlet boundary pressure is extrapolated from interior domain, velocity and temperature is set equal to the free-stream values. Both velocity and temperature fields are considered to be developing. At the outlet boundary the pressure is fixed and the remaining variables are interpolated from interior domain.

### Grid Features

To have a smooth grid an elliptic method has been applied. Grids have been clustered in regions with large gradients of variables to improve the efficiency as shown in Figure 1. The developed methods had been applied to different grid resolutions such as 80*30, 100*40, 120*40 and 160*60 to ensure grid independency of results. Grid independency has been achieved in 120*40 resolution as shown in figure 2. All the results reported in the present work are based on 120*40 grid size.

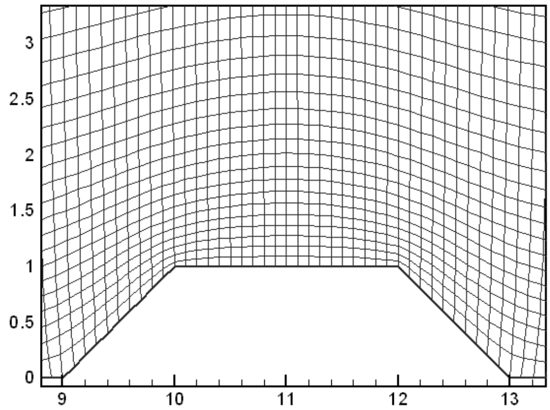


Figure 1. A part of grid generated for semi-hexagonal riblet

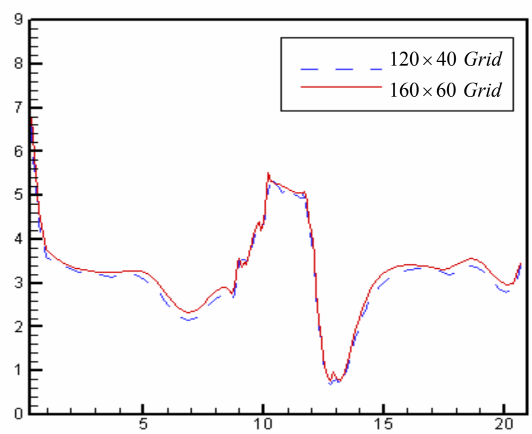


Figure 2. Grid independency by comparing Nusselt number

**Numerical Results**

Validation of the method was attained by performing calculations for the case of flow with one rectangular riblet attached to the lower wall with constant heat flux, for which the numerical results exist in the literature. Figure 3, compares the results of present work with those of Ref [17] for local Nusselt number. A quite good agreement is observed between the two solutions.

All the numerical results demonstrated, have been obtained from a solver written by the authors. This solver is equipped by three flux calculation models, namely Jameson flux averaging, first and second-order developed methods. ACM was successfully applied in proceeding methods. Several numerical tests were conducted in different Reynolds numbers and for various geometries. The results for semi-hexagonal case are presented here because there was little data about this shape of riblet in literature.

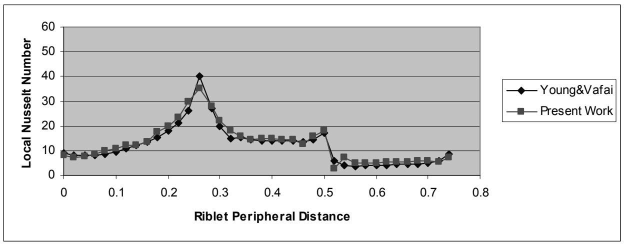


Figure 3. Comparing results of present results with those of Ref [17]

For design purposes Nusselt number is an important factor so local Nusselt numbers are represented for different Reynolds numbers and also for three different method of calculating convective fluxes, in Figure 4. As can be seen, at the leading edge of the surface the flow is developing so local Nusselt number is high until it reaches forward stagnation point of the riblet, where the Nusselt number decreases. At the first vertex of riblet because of high mixing effect Nuselt number rises. Another extremum can be seen at the second vertex of riblet. Behind the riblet again because of the stagnation effect Nusselt number decreases.

To have a better understanding of the Nusselt number behavior and also showing the ability of the developed method in modeling the velocity field, velocity vectors and stream lines for second-order method in Re=100 are presented in Figures 5-6. As can be observed in region behind the riblet the vorticity region is clearly noticeable.

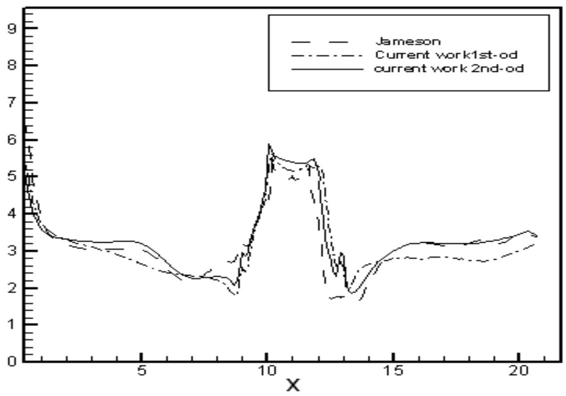


Figure 4.a. Local Nusselt Number for the three methods in Re=30, Pr=0.71, CFL=0.6

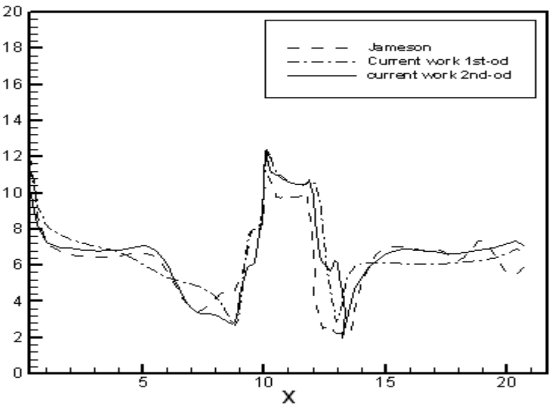


Figure 4.b. Local Nusselt Number for the three methods in Re=100, Pr=0.71, CFL=0.6

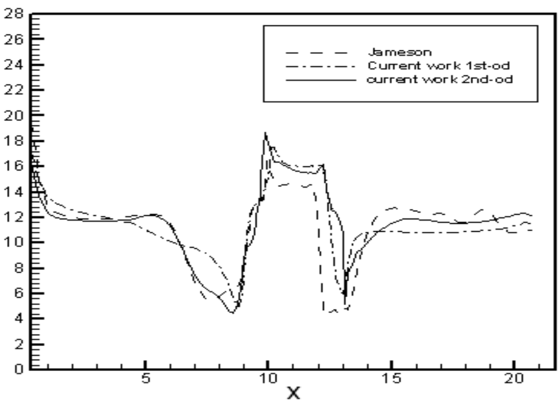


Figure 4.c. Local Nusselt Number for the three methods in Re=200, Pr=0.71, CFL=0.6

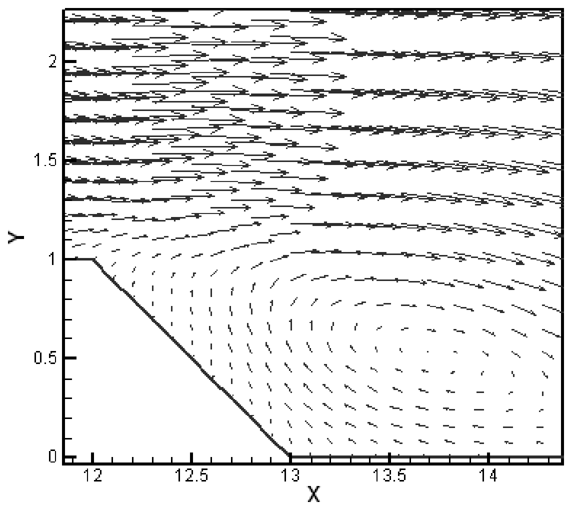


Figure 5. Velocity Vectors behind the Riblet, Re=100, CFL=0.6

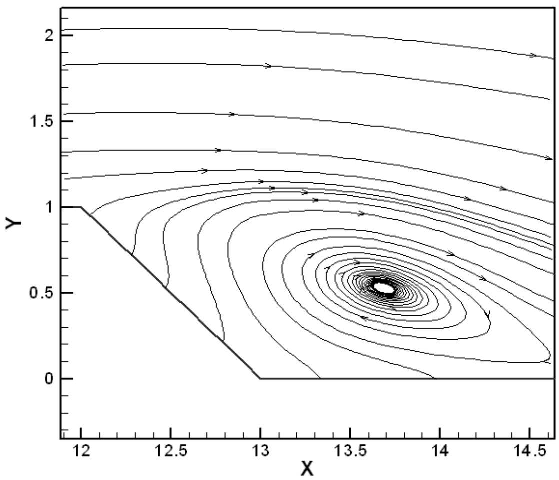

Figure 6. Streamlines behind the Semi-hexagonal riblet, Re=100, CFL=0.6

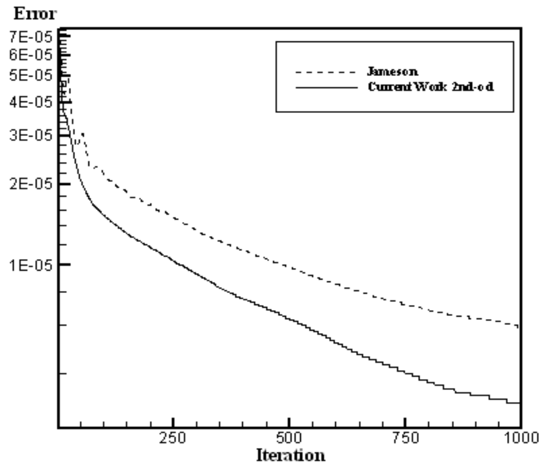

Figure 7. Comparison between Jamesons Flux averaging and present 2nd-order methods convergence rates, Re=200, CFL=0.6

One of the most important properties of a method is its convergence rate. According to figure 7, the proposed method has a much better convergence rate. For example to reach an error of e-5, 480 iterations in averaging method and 280 iterations in the proposed method, is required

## Concluding Remarks

A Roe-like Characteristic based, high order method was developed to solve velocity and temperature fields simultaneously in a new geometry. The enhanced method was quite successful in predicting both the velocity and temperature fields over a semi-hexagonal riblet in different Reynolds numbers. The convergence rate of the method is reported in Figure 7, In which the proposed second-order Roe-like method demonstrates a better convergence rate. This was partly due to the second-order upwind flux treatment and also employing the fifth-order Runge-Kuta algorithm. This kind of flux treatment relates the physical flow behaviour to the mathematics in a genuinely approach. The flux treatment considers the virtual acoustic wave propagation in the computational domain. This is made possible, by reconstruction of fluxes and their corresponding eigenvectors. By the aid of ACM the governing equations took a hyperbolic dominated nature, therefore the application of characteristic based wave propagation models would become possible.

## References


[1] Briley, W. & Neerarambam, S., Implicit Lower-upper/Approximate-factorization Schemes for Incompressible Flows, J. Comp. Phys. Vol. 128, 1996, pp. 32.

[2] Chorin, A.J., A Numerical Method for Solving Incompressible Viscous Flow Problems, J. Comp. Phys., Vol. 2, Aug. 1967, pp. 12-26.

[3] Drikakis, D. & Rider, W., High-resolution Methods for Incompressible and Low- Speed Flows, Springer, 2004.

[4] Hartwich, P. & Hsu, C., High Resolution Upwind Schemes for the Three-dimensional Incompressible Navier-Stokes Equations, AIAA 87-0547, 1987.

[5] Hong, Y.J., Hsieh, S.S. & Shih, H.J., Numerical Computation of laminar Separation and Reattachment of Flow over Surface-Mounted Ribs, J. Fluids Eng., Vol. 133(6), 1991, pp. 190-198.

[6] Jameson, A., Analysis and Design of Numerical Schemes for Gas Dynamics 1 Artificial Diffusion, Upwind Biasing, Limiters and Their Effect on Accuracy and Multi-grid Convergence, Int. J. Comp. Flu. Dynamics, V4, pp. 171-218.

[7] Kao, P.H. & Yang, R.J., A Segregated-Implicit Scheme for Solving the Incompressible Navier-Stokes Equations, J. Computers and Fluids, 2007.

[8] Liou, T.M. & Kao, C.W., Chen, S.H., Flowfield Investigation of the Effect of Rib Open Area ratio in a Rectangular Duct, J. Fluids Eng., Vol. 120, pp. 504-512.

[9] Madsen, P. A. & Schaffer, H. A., A Discussion of Artificial Compressibility, J. Costal Engineering, Vol. 53, 2006, pp. 93-98.

[10] McClimans, T.A., Pietrzak, J.D., Huess, V., Nilsen, N. & Johannessen, B.O., Laboratory and Numerical Simulation of the Skagerrak Circulation, Cont. Shelf Res. 20, 2000, 941-974.

[11] Powell, K.G., VanLeer, B. & Roe, P., Towards a Genuinely Multi-Dimensional Upwind Scheme, Von Karman Institute for fluid Dynamics, Lecture Series 1990- 03, March 1990.

[12] Rogers, S.E. & Kwak, D., Upwind differencing scheme for the time-accurate Incompressible Equations, AIAA J., Vol. 28, 1990, pp. 253-262.

[13] Rogers, S.E., Kwak, D. & Krisis, C., Steady and Unsteady Solutions of the Incompressible Navier-Stokes Equations, AIAA journal, Vol. 29, 1991, pp. 603-610.

[14] Tai, C.H., Zhao, Y. & Liew, K.M., Parallel Computation of Unsteady Three-dimensional Incompressible Viscous Flow Using an Unstructured Multi-Grid Method, J. Computers and Structures, vol. 82, 2004, pp. 2425-2436.

[15] Volpe, G., On the Use and Accuracy of Compressible Flow Codes at Low Mach Numbers, AIAA 91-1662, 1991.

[16] Yang, J.Y., Yang, S.C., Chen, Y.N. & Hsu, C.A., Implicit Weighted ENO Schemes for Three-dimensional Incompressible Navier-Stokes Equations, J. Comp. Phys., Vol. 146, 1998, pp. 464.

[17] Vafai, K. & Young, T.J., Convective Cooling of Heated Obstacle in a channel, J. Heat and Mass Transfer, Vol.41, 1998, pp. 3131-3148.

| **Nomenclature** | |
|---|---|
| $A$ | dimensionless flux jacobian matrix |
| $CFL$ | Courant number |
| $F, G$ | dimensionless flux vector components |
| $L$ | dimensionless Left eigen vector |
| $N$ | dimensionless normal velocity |
| $NF$ | dimensionless normal flux |
| $Nu$ | Nusselt number |
| $n_x, n_y$ | grids normal vector components |
| $p$ | dimensionless pressure |
| $\hat{p}$ | pressure, Pa |
| $\Pr$ | Prandtl number |
| $R, S$ | dimensionless viscous flux components |
| $R$ | dimensionless right eigen vector |
| $\mathrm{Re}$ | Reynolds number |
| $t$ | dimensionless time |
| $\hat{t}$ | time, s |
| $T$ | temperature, k |
| $u, v$ | dimensionless velocity components |
| $\hat{u}, \hat{v}$ | velocity components, m/s |
| $x, y$ | dimensionless coordinates |
| $\hat{x}, \hat{y}$ | physical coordinates |
| $\alpha$ | thermal diffusivity, $m^2/s$ |
| $\beta$ | artificial compressibility, dimensionless |
| $\theta$ | dimensionless temperature |
| $\rho$ | $kg/m^3$ density, |
| $\lambda$ | eigen values |
| $\Lambda$ | matrix of eigen values |
| $\varphi$ | shear velocity |
| $\nu$ | $m^2/s$ kinematic viscosity, |
| $\Omega$ | dimensionless cell area |

| subscripts | |
|---|---|
| $\infty$ | free stream values |
| $w$ | wall |
| R | right |
| L | left |